Article

A Quantum Chemical Study of the Reaction Mechanism of Acetyl-Coenzyme A Synthase

Patricia Amara, Anne Volbeda, Juan Carlos Fontecilla-Camps, and Martin J. Field

J. Am. Chem. Soc., **2005**, 127 (8), 2776-2784• DOI: 10.1021/ja0439221 • Publication Date (Web): 05 February 2005

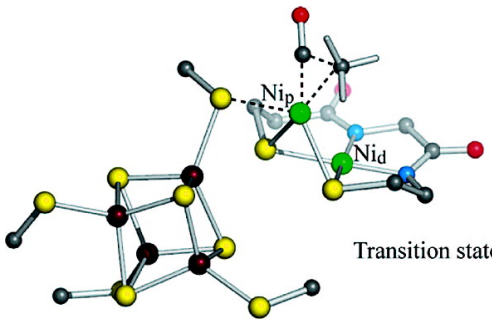

Transition state for acetyl formation in ACS

More About This Article

Additional resources and features associated with this article are available within the HTML version:

- Supporting Information
- Links to the 7 articles that cite this article, as of the time of this article download
- Access to high resolution figures
- Links to articles and content related to this article
- Copyright permission to reproduce figures and/or text from this article

View the Full Text HTML

J|A|C|S
ARTICLES
Published on Web 02/05/2005

A Quantum Chemical Study of the Reaction Mechanism of Acetyl-Coenzyme A Synthase

Patricia Amara,[†] Anne Volbeda,[‡] Juan Carlos Fontecilla-Camps,[‡] and Martin J. Field*,[†]

Contribution from the Laboratoire de Dynamique Moléculaire and [‡]Laboratoire de Cristallographie et Cristallogenèse des Protéines, Institut de Biologie Structurale − Jean-Pierre Ebel, CEA/CNRS/UJF, 41, rue Jules Horowitz, F-38027 Grenoble Cedex 01, France

Received October 6, 2004; E-mail: mjfield@ibs.fr

Abstract: Recent experimental and theoretical studies have focused on the mechanism of the A-cluster active site of acetyl-CoA synthase that produces acetyl-CoA from a methyl group, carbon monoxide, and CoA. Several proposals have been made concerning the redox states of the (Ni−Ni) bimetallic center and the iron−sulfur cluster connected to one of the metals. Using hybrid density functional theory, we have investigated putative intermediate states from the catalytic cycle. Among our conclusions are the following: (i) the zerovalent state proposed for the proximal metal is unlikely if the charge on the iron−sulfur cluster is +2; (ii) a mononuclear mechanism in which both CO and CH_3 bind the proximal nickel is favored over the binuclear mechanism in which CO and CH_3 bind the proximal and distal nickel ions, respectively; (iii) the formation of a disulfide bond in the active site could provide the two electrons necessary for the reaction but only if methylation occurs simultaneously; and (iv) the crystallographic closed form of the active site needs to open to accommodate ligands in the equatorial site.

Introduction

Acetyl-CoA synthase (ACS) complexed with carbon monoxide dehydrogenase (CODH) catalyzes (1) the reversible reduction of CO_2 to CO at the C-cluster of CODH and (2) the synthesis of acetyl-CoA from a methyl group of a corrinoid-iron-sulfur-protein (CoFeSP), CO, and CoA at the A-cluster of ACS:

$$CO_2 + 2H^+ + 2e^- \rightleftharpoons CO + H_2O \quad (1)$$

$$CH_3^+ + CO + CoA\text{-}S^- \rightleftharpoons CoA\text{-}S(CO)CH_3 \quad (2)$$

Experiments revealing that CO produced at the C-cluster was not found in solution led to the conclusion that CO had to reach the A-cluster from the interior of the ACS/CODH complex.[1,2] Indeed, the first X-ray structure of this bifunctional enzyme complex from *Moorella thermoacetica* (formerly known as *Clostridium thermoaceticum*) confirmed the presence of a hydrophobic tunnel network that provided a potential route for CO synthesized from CO_2 at the C-cluster to reach the A-cluster.[3] However, in this structure, the A-cluster appeared to be inaccessible for coenzyme A and the CoFeSP. A second X-ray structure showed that the three domains of the ACS subunit may adapt two different conformations: a closed one similar to that observed in the first structure, and an open one, in which the A-cluster is exposed at the surface.[4] In the open conformation, however, CO access from the C-cluster to the A-cluster is prevented by the movement of an α-helix which blocks the tunnel, and consequently, the authors proposed a functional role for this conformational change that would regulate the accessibility of the A-cluster to CO. More recently, a very similar open conformation was observed in the crystal structure of the monomeric ACS of *Carboxydothermus hydrogenoformans*.[5]

The A-cluster active site consists of an $[Fe_4S_4]$ cluster connected to a proximal metal site (denoted with the p index) by a bridging cysteine. This metal is connected via two other bridging cysteines to a distal metal (denoted with the d index), which, in turn, is coordinated to two nitrogen atoms from the protein backbone. While the identity of the distal metal was determined to be nickel from X-ray anomalous scattering experiments, three different metals were found at the proximal site: Cu[3] and Zn[4] in the closed form of ACS and Ni in the open form.[4,5] When the first structure of the ACS/CODH complex was published,[3] the authors reported that the Cu_p−Ni_d center was active, a result which they later confirmed.[6] In light of the second complex structure[4] and other studies,[5,7,8] the

[†] Laboratoire de Dynamique Moléculaire.
[‡] Laboratoire de Cristallographie et Cristallogenese des Protèines.

(1) Maynard, E. L.; Lindahl, P. A. *J. Am. Chem. Soc.* **1999**, *121*, 9221−9222.
(2) Seravalli, J.; Ragsdale, S. W. *Biochemistry* **2000**, *39*, 1274−1277.
(3) Doukov, T. I.; Iverson, T. M.; Seravalli, J.; Ragsdale, S. W.; Drennan, C. L. *Science* **2002**, *298*, 567−572.
(4) Darnault, C.; Volbeda, A.; Kim, E. J.; Legrand, P.; Vernède, X.; Lindahl, P. A.; Fontecilla-Camps, J. C. *Nat. Struct. Biol.* **2003**, *10*, 271−279.
(5) Svetlitchnyi, V.; Dobbek, H.; Meyer-Klaucke, W.; Meins, T.; Thiele, B.; Römer, P.; Huber, R.; Meyer, O. *Proc. Natl. Acad. Sci. U.S.A.* **2004**, *101*, 446−451.
(6) Seravalli, J.; Gu, W.; Tam, A.; Strauss, E.; Begley, T. P.; Cramer, S. P.; Ragsdale, S. W. *Proc. Natl. Acad. Sci. U.S.A.* **2003**, *100*, 3689−3694.
(7) Bramlett, M. R.; Tan, X.; Lindahl, P. A. *J. Am. Chem. Soc.* **2003**, *125*, 9316−9317.
(8) Gencic, S.; Grahame, D. A. *J. Biol. Chem.* **2003**, *278*, 6101−6110.

10.1021/ja0439221 CCC: $30.25

Ni_p-Ni_d center was shown to be active, not the Cu_p-Ni_d and Zn_p-Ni_d sites. Ragsdale and co-workers, who first believed in the functional role of copper, have now also come round to the conclusion that the structure with copper is inactive.[9] Ni_d has a square planar conformation in all crystallographic structures, whereas M_p has a square planar geometry in the open form of the protein (Ni_p) and a tetrahedral coordination in the closed form (Zn_p and Cu_p).

An overview of the catalytic mechanisms that have been proposed for the active form of ACS has recently been given by Hegg,[10] so we do not describe them in detail here. The main proposals, based upon experimental evidence, are those from Doukov et al.,[3,6] from Darnault et al.,[4] and from Gencic and Grahame.[8] There are significant doubts about many aspects of the mechanism, and we highlight a number of them in what follows.

(1) The overall reaction 2 does not produce or consume electrons, but formation of a stable methylated A-cluster, which is presumed to be an intermediate in the catalytic cycle, requires two electrons to form the metal−methyl bond. This is because the methyl group is donated by CoFeSP as a cation.[11] Before the first crystal structure was solved, Lindahl and co-workers proposed the existence of a pair of cysteines in ACS, denoted the D-site, which could deliver two electrons to the A-cluster upon disulfide-bond formation.[12] No such site was found outside the A-cluster in the crystal structures, but Meyer and co-workers proposed that a disulfide bond might be formed by the two Ni_p/Ni_d-bridging cysteine thiolates.[5] Alternative proposals have assigned the electron-donor role to other parts of the A-cluster, such as (i) a fully reduced $[Fe_4S_4]^0$ cluster;[27] (ii) a reduced $[Fe_4S_4]^{1+}$ cluster in combination with a monovalent Ni ion (either Ni_p or Ni_d), each of which could provide one electron;[6,8] and (iii) Ni_p.[4,13] according to the latter proposal, the active enzyme would actually contain a zerovalent $Ni_p(0)$ which converts to $Ni_p(II)$ upon binding of the methyl group. This unusual oxidation state for nickel was questioned by theoretical work that found the electronic state $[Fe_4S_4]^{1+}-Ni_p(I)$ to be favored over $[Fe_4S_4]^{2+}-Ni_p(0)$.[14] However, there is experimental evidence that redox changes of the $[Fe_4S_4]$ cluster are much slower than the turnover rate of the enzyme,[15] suggesting that it remains in the same oxidation state during the whole catalytic cycle.[4]

(2) The ACS active site should contain binding sites for two one-carbon substrates. Ragsdale and co-workers suggested a binuclear mechanism in which the CO and the CH_3 bind to Cu_p and Ni_d, respectively.[3,6] Others have proposed that a single nickel be the binding site for both substrates.[4,8] An electron-donor role for Ni_d, required for methyl binding, is questionable because its square planar coordination favors a low spin Ni(II) state. In addition, the crystal structures show it to be less accessible than Ni_p to the CoFeSP.

(3) The sequence of reaction steps is unclear, and there is a debate concerning whether CO[3,4,16] or CH_3 [8,13] binds first. In vitro, the reaction may proceed either by first exposing the enzyme to externally added CO, followed by methyl binding,[17] or the other way around,[12] before adding CoA. In vivo, CO probably reaches the A-cluster through the internal tunnel that connects it to the C-cluster, and this is likely to favor one of the two possible reaction sequences. The tunnel connects the C-cluster to the A-cluster only in the closed form of ACS, and it exits at an apical ligand site of the proximal metal, M_p. Other ligand positions are sterically blocked because the A-cluster is buried in the closed form. In contrast, the A-cluster lies exposed at the surface of the protein in the open form of ACS, and so the equatorial site of Ni_p is accessible. Based on these observations, it was proposed that the most likely reaction sequence starts with binding of CO to the apical ligand site of Ni_p in the closed form of the enzyme, followed by a transition to the open form allowing transfer of the methyl group from CoFeSP to a vacant equatorial ligand site.[4,16]

(4) The so-called NiFeC (or A_{red}-CO) species is detected by EPR spectroscopy when CO is added to the enzyme. Its structure is unknown, and it is uncertain whether it is actually part of the catalytic cycle[3,6,17] or not.[4,8,12] Experiments are ambivalent as to whether there are EPR-active species, such as NiFeC, in the catalytic cycle, and so there may be doubts about mechanisms that invoke them.

One way to address the above questions is to analyze putative reaction intermediates and transition states by subjecting them to a quantum chemical analysis. Previous theoretical work on the A-cluster has concentrated on modeling of the NiFeC state,[14,18] the catalytic relevance of copper and a possible zero oxidation state for Ni_p.[14] More recently, another theoretical study on a constructed model of the A-cluster discussed the relevance of copper and proposed a mechanism.[19]

In this work, we have modeled different states that could possibly be adopted by the A-cluster and confronted these with available experimental data. The structural and electronic configurations of the models were investigated using density functional theory (DFT) calculations. We have concentrated on the proposed mechanism of Darnault et al.,[4] shown in Figure 1, but we also examined proposals by other groups.

Modeling the Active Site

Methods. All quantum chemical calculations were done using the program Jaguar.[20] We employed a DFT method with the B3LYP functional and the LACVP** basis set. This combination has given good structural results for other metal-containing systems.[21] A larger basis set, consisting of the LACV3P** basis for metal atoms and the cc-pVTZ(-F) basis for other atoms, was used for single-point energy calculations at geometry-optimized structures. The antiferromagnetic couplings present in the system were modeled using spin-unrestricted DFT and Jaguar's powerful set of broken symmetry methods. These methods allow us to model the iron−sulfur cluster in both its $[Fe_4S_4]^{2+}$ and $[Fe_4S_4]^{1+}$ forms. The former is modeled as 2 Fe^{3+}($s = 5/2$) and 2

(9) Seravalli, J.; Xiao, Y.; Gu, W.; Cramer, S. P.; Antholine, W. E.; Krymov, V.; Gerfen, G. J.; Ragsdale, S. W. *J. Am. Chem. Soc.* **2004**, *43*, 3944−3955.
(10) Hegg, E. L. *Acc. Chem. Res.* **2004**, ASAP.
(11) Menon, S.; Ragsdale, S. W. *Biochemistry* **1998**, *37*, 5689−5698.
(12) Barondeau, D. P.; Lindahl, P. A. *J. Am. Chem. Soc.* **1997**, *119*, 3959−3970.
(13) Lindahl, P. *JBIC* **2004**, *9*, 516−524.
(14) Schenker, R. P.; Brunold, T. C. *J. Am. Chem. Soc.* **2003**, *125*, 13962−13963.
(15) Tan, X.; Sewell, C.; Yang, Q.; Lindahl, P. A. *J. Am. Chem. Soc.* **2003**, *125*, 318−319.
(16) Volbeda, A.; Fontecilla-Camps, J. C. *JBIC* **2004**, *9*, 525−532.
(17) Seravalli, J.; Kumar, M.; Ragsdale, S. W. *Biochemistry* **2002**, *41*, 1807−1819.
(18) Craft, J. L.; Mandimutsira, B. S.; Fujita, K.; Riordan, C. G.; Brunold, T. C. *Inorg. Chem.* **2003**, *42*, 859−867.
(19) Webster, C. E.; Darensbourg, M. Y.; Lindahl, P. A.; Hall, M. B. *J. Am. Chem. Soc.* **2004**, *126*, 3410−3411.
(20) Jaguar 5.5, Schrödinger, L.L.C.: Portland, OR, 1991−2003.
(21) Wirstam, M.; Lippard, S. J.; Friesner, R. A. *J. Am. Chem. Soc.* **2003**, *125*, 3980−3987.

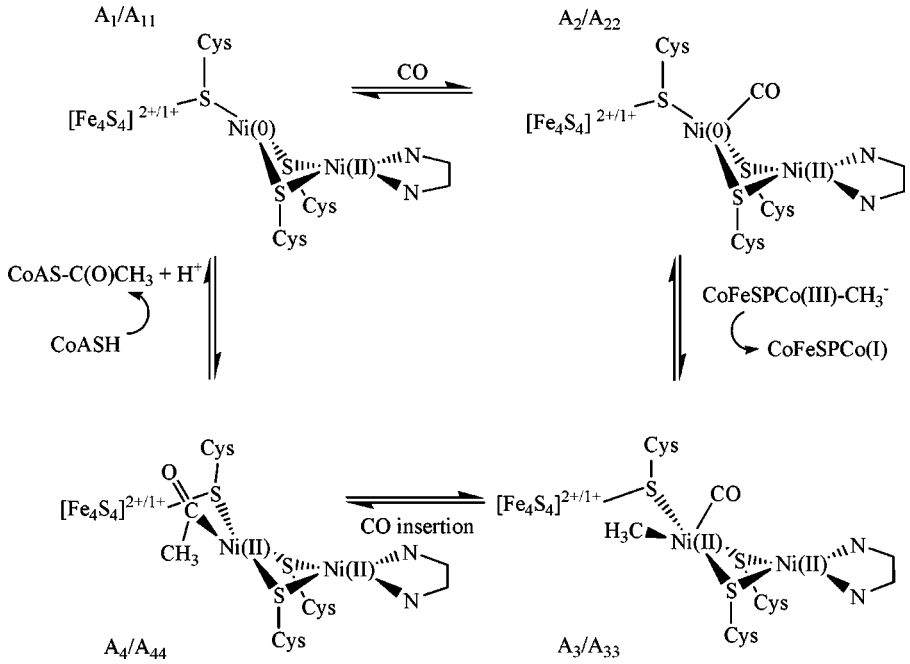

Figure 1. Proposed mechanism from ref 4 tested in the present study.

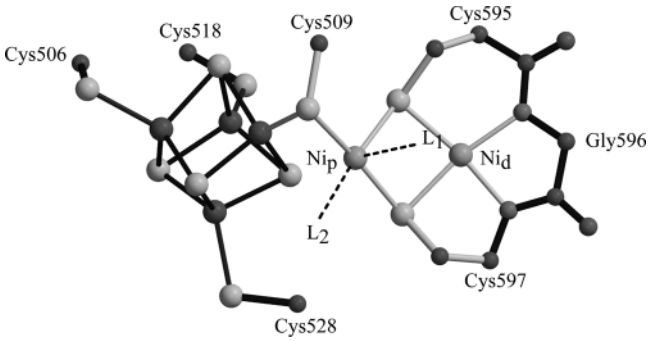

Figure 2. Basic model of the active site of the A-cluster used for all quantum chemical calculations. Hydrogens were added to block the cysteines and the glycine. Bonds in light gray connect the atoms that are allowed to move during geometry optimization. The dashed lines point to two ligand binding sites of Ni_p: L_1 (ax) and L_2 (eq).

$Fe^{2+}(s = 2)$ with both $Fe^{3+}-Fe^{2+}$ pairs antiferromagnetically coupled and the latter by 1 $Fe^{3+}(s = 5/2)$ and 3 $Fe^{2+}(s = 2)$ with the $Fe^{3+}-Fe^{2+}$ and $Fe^{2+}-Fe^{2+}$ pairs antiferromagnetically coupled.[22] Atomic charge and spin population analyses for all calculations were performed using the standard methods in Jaguar.

Active Site Models. All calculations were performed using the basic A-cluster model of the active site shown in Figure 2. We modeled a number of states from the catalytic cycle, and for some of these, additional ligands were added at the axial (ax) and equatorial (eq) sites of Ni_p. These correspond to positions L_1 and L_2 in Figure 2, respectively. The geometries of both active site conformers of the A-cluster in the X-ray structure of Darnault et al.[4] were used as starting points in our study. The open form contains a Ni−Ni metal site, but the closed form has a Zn−Ni metal site. We replaced the Zn by Ni in our calculations, as it is now known that the active A-cluster contains a Ni−Ni center.[4,5,7−9]

We did not include the protein matrix in our study, in part due to computational cost. This is a simplification, but quantum chemical studies of model compounds have given useful insights about the mechanisms of several enzymes.[23,24] One of the most important effects of the protein matrix is that it prevents certain structural changes from occurring. To mimic this effect, we only allowed the nickel atoms and their cysteine and nonproteic ligands to move in all geometry optimizations. We tested this approximation by performing some calculations without geometrical constraints on the $[Fe_4S_4]$ cluster and found that their electronic structures and their geometries did not change significantly. On the other hand, releasing constraints on all atoms sometimes led to structural changes that are precluded within the protein matrix. Calculations which include the environment in some way, such as via hybrid quantum mechanical (QM)/molecular mechanical (MM) potentials,[25,26] could be used to address some of these limitations. The complexity of the ACS system and the efficiency of current QM/MM methods are such though that these type of calculations would be very challenging.

Results and Discussion

Our modeling concentrated on four aspects of the behavior of the A-cluster: the nature of the NiFeC species, the redox states available to the nickel atoms in the active site during the initial stages of the catalytic cycle, acetyl formation, and the possibility of a D-site. We discuss each of these in turn, but the results for the models that we considered are summarized in Tables 1−4. Table 1 lists the formal properties of the A-cluster models, whereas the other three give key distances for the geometry-optimized structures and the results of the charge and spin analyses, respectively.

NiFeC Species. We considered three possible configurations for the NiFeC state. Our first model, $NiFeC_1$, consists of a closed-form structure with a tetrahedral-$Ni_p(I)$/square planar-$Ni_d(II)$ pair and an $[Fe_4S_4]^{2+}$ cluster.[13] A model with such an electronic configuration is stable and is maintained during geometry optimization. Spin analysis shows that most of the spin is located on the tetrahedral Ni_p (0.89) and that the cluster remains oxidized, whereas Ni_d bears no significant spin density. Some spin density is observed on the cysteine thiolates bound

(22) Xia, J.; Hu, Z.; Popescu, C. V.; Lindahl, P. A.; Münck, E. *J. Am. Chem. Soc.* **1997**, *119*, 8301−8312.
(23) Friesner, R. A.; Dunietz, B. D. *Acc. Chem. Res.* **2001**, *34*, 351−358.
(24) Siegbahn, P. E. M.; Blomberg, R. A. *Chem. Rev.* **2000**, *100*, 421−437.
(25) Amara, P.; Field, M. J. In *Computational Molecular Biology*; Leszczynski, J., Ed.; Elsevier: Amsterdam, 1999; pp 1−33.
(26) Gao, J.; Truhlar D. G. *Annu. Rev. Phys. Chem.* **1991**, *53*, 467−505.

Table 1. Theoretical Models of the A-cluster[a]

models	charge	spin	conformation	Ni_p	Ni_p ligand	Ni_d	Ni_d ligand	Fe_4S_4	S–S bond	final state
A_{ox}	−2	0	closed	II		II		+2		same
A_1	−4	0	closed	0		II		+2		$[Fe_4S_4]^{1+}$ ($s = {}^1/_2$) Ni_p(I) ($s = -{}^1/_2$)
A_{11}	−5	$^1/_2$	closed	0		II		+1		same
A_2	−4	0	closed	0	CO^{ax}	II		+2		$[Fe_4S_4]^{1+}$($s = {}^1/_2$) Ni_p(I) ($s = -{}^1/_2$)
A_{22}	−5	$^1/_2$	closed	0	CO^{ax}	II		+1		same
A_2'	−3	0	open	II	CH_3^{eq}	II		+2		same
A_3	−3	0	open	II	CH_3^{eq} and CO^{ax}	II		+2		same
A_3'	−3	0	open	II	CO^{ax}	II	CH_3	+2		$[Fe_4S_4]^{1+}$ ($s = {}^1/_2$) Ni_p(III) ($s = -{}^1/_2$) CO^{eq}
A_4	−3	0	open	II	CH_3CO^{eq}	II		+2		same
A_4''[b]	−3	0	open	II	CH_3CO^{eq}	II		+2		same
disu1	−2	0	open	0		II		+2	$S_{Cys528}-S_{Cys597}$	A_{ox}
disu2	−2	0	open	0		II		+2	$S_{Cys528}-S_{Fe4S4}$	A_{ox}
$NiFeC_1$	−3	$^1/_2$	closed	I	CO^{ax}	II		+2		same
$NiFeC_2$	−3	$^1/_2$	closed	II	radical CO^{ax}	II		+2		$NiFeC_1$
$NiFeC_3$	−3	$^1/_2$	open	II	radical CO^{eq}	II		+2		$[Fe_4S_4]^{1+}$ ($s = {}^1/_2$) Ni_p(II) nonradical CO

[a] For each model, the total charge and spin, the formal charges of the metals Ni_p and Ni_d and any ligand or disulfide bonds are indicated. The final state is indicated where the geometry optimization led to a different electronic configuration [b] CH_3CO orientation changes dihedral $S_{Cys509}-Ni_p-C_{CO}-C_{CH_3} = -86°$ (instead of +73° in A_4).

Table 2. Key Distances, in Å, for the X-ray Structures and the Optimized Models[a]

models	Ni_p–Ni_d	Ni_p–S_{595}	Ni_p–S_{597}	Ni_p–S_{509}	Fe–S_{509}	Ni_p ligand	Ni_d ligand	Ni_d–S_{595}	Ni_d–S_{597}
closed (Zn_p)	2.83	2.34	2.34	2.37	2.26	SO? = 2.28		2.23	2.20
open (Ni_p)	3.00	2.37	2.18	2.26	2.32	$CH_3CO_2^-$? = 2.44		2.23	2.27
A_{ox}	2.77	2.28	2.28	2.28	2.48			2.24	2.30
A_1	3.05	2.39	2.33	2.30	2.48			2.26	2.30
A_{11}	3.06	2.49	2.41	2.34	2.46			2.25	2.29
A_2	2.92	2.45	2.40	2.38	2.48	CO = 1.92		2.26	2.29
A_{22}	2.96	2.53	2.53	2.57	2.42	CO = 1.69		2.24	2.27
A_2'	3.07	2.39	2.27	2.28	2.43	CH_3 = 1.96		2.25	2.24
A_3	3.04	2.42	2.35	2.35	2.39	CO = 1.97, CH_3 = 1.98		2.25	2.26
A_3'	3.24	2.57	2.43	2.38	2.51	CO = 1.86	CH_3 = 1.99	2.22	2.26
A_4	3.03	2.41	2.28	2.27	2.44	CH_3CO = 1.89		2.25	2.26
A_4'	3.05	2.41	2.27	2.27	2.42	CH_3CO = 1.88		2.26	2.25
$NiFeC_1$	2.99	2.43	2.39	2.41	2.40	CO = 1.83		2.26	2.29
$NiFeC_3$	3.04	2.30	2.31	2.29	2.52	CO = 1.82		2.24	2.25

[a] The terms "closed (Zn_p)" and "open (Ni_p)" refer to the X-ray structures of ref 4. Model $NiFeC_2$ is omitted as it optimizes to the model $NiFeC_1$.

Table 3. Atomic Charge Populations, Resulting from a Mulliken Analysis, of the Main Atoms in the Active Site for Each Optimized Model

models	S_{506}	S_{518}	S_{528}	Fe_4S_4	S_{509}	Ni_p	CO	CH_3	CH_3CO	S_{595}	S_{597}	Ni_d
A_{ox}	−0.19	−0.15	−0.20	−0.74	−0.09	−0.04				0.09	0.03	0.26
A_1	−0.51	−0.49	−0.50	−0.77	−0.36	0.13				−0.16	−0.16	0.26
A_{11}	−0.52	−0.49	−0.52	−0.97	−0.29	−0.57				−0.16	−0.18	0.32
A_2	−0.50	−0.49	−0.50	0.20	−0.30	−0.00	−0.14			−0.08	−0.11	0.27
A_{22}	−0.53	−0.50	−0.52	−0.86	−0.28	−0.20	−0.39			−0.12	−0.15	0.22
A_2'	−0.45	−0.40	−0.41	−0.20	−0.22	0.03		−0.25		−0.07	−0.06	0.37
A_3	−0.45	−0.40	−0.42	−0.17	−0.18	−0.15	0.04	−0.20		−0.03	−0.06	0.34
A_3'	−0.47	−0.46	−0.45	−0.60	−0.28	−0.05	−0.03	0.04		0.03	0.00	0.41
$A_4' \approx A_4$	−0.45	−0.41	−0.40	−0.17	−0.24	−0.01			−0.27	−0.05	−0.06	0.36
$NiFeC_1$	−0.44	−0.42	−0.44	−0.16	−0.27	0.02	−0.10			−0.12	−0.16	0.32
$NiFeC_3$	−0.47	−0.46	−0.44	−0.58	−0.20	−0.09	0.08			0.05	−0.05	0.37

to the cluster (Cys506, Cys518, and Cys528). The $[Fe_4S_4]^{2+}$ cluster itself has very little net spin and has a typical ($^9/_2$, $-{}^9/_2$) spin distribution.

Schenker and Brunold performed a similar calculation starting from the X-ray structure of reference[3] and replacing Cu_p by Ni_p.[14] In their model, most of the spin was on Ni_p (0.43), but Ni_d and the $[Fe_4S_4]$ cluster, combined with its four cysteine ligands, had nonnegligible spin densities of 0.26 and 0.20, respectively. The Ni_p-Ni_d distance in their structure was 2.60 Å, which is much closer to the Cu_p-Ni_d distance of 2.65 Å found by EXAFS[6] than to the distance of 2.80 Å found by X-ray crystallography.[3] This value is also shorter than the Ni_p-Ni_d distance of 3.00 Å found by X-ray crystallography[4] and the distances of 2.96 and 2.80 Å found by EXAFS for the as-isolated and the Ti^{3+}-reduced forms of the A-cluster from acetyl-CoA decarbonylase/synthase (ACDS), respectively.[27] In contrast, we find a Ni_p-Ni_d distance of 2.99 Å which is in good agreement with the available experimental values. We also find a Ni_p-CO distance of 1.83 Å which compares to the value from Schenker and Brunold's structure of 1.74 Å. To examine the

(27) Gu, W.; Gencic, S.; Cramer, S. P.; Grahame, D. A. *J. Am. Chem. Soc.* **2003**, *125*, 15343−15351.

Table 4. Atomic Spin Populations, Resulting from a Mulliken Analysis, of the Main Atoms in the Active Site for Each Optimized Model

models	S_{506}	S_{518}	S_{528}	Fe_4S_4	S_{509}	Ni_p	CO	CH_3	CH_3CO	S_{595}	S_{597}	Ni_d
A_{ox}	0.26	−0.33	0.25	−0.08	0.07	−0.44				0.12	−0.02	0.16
A_1	0.13	−0.11	0.14	0.89	−0.06	−0.95				−0.05	0.01	−0.01
A_{11}	0.12	−0.10	0.13	1.10	−0.06	−0.10				−0.04	0.02	−0.10
A_2	0.13	−0.11	0.15	0.85	−0.11	−0.92	0.07			−0.03	−0.03	−0.01
A_{22}	0.11	−0.10	0.13	0.92	−0.07	−0.01	0.00			−0.01	0.01	0.00
A_2'	0.18	−0.23	0.20	−0.03	−0.07	−0.06		0.00		0.00	0.00	0.00
A_3	0.18	−0.23	0.20	−0.04	−0.06	−0.03	−0.03	−0.01		−0.01	0.03	0.00
A_3'	0.16	−0.12	0.16	0.91	−0.11	−0.86	0.01	0.01		−0.03	−0.05	−0.13
$A_4' \approx A_4$	0.18	−0.23	0.20	−0.06	−0.07	−0.05			0.00	0.00	0.00	0.00
$NiFeC_1$	0.18	−0.23	0.19	−0.04	−0.03	0.89	−0.05			0.03	0.05	0.00
$NiFeC_3$	0.16	−0.14	0.17	0.72	0.01	0.05	0.02			−0.03	0.03	0.00

discrepancy between these two sets of results, we performed calculations on the structure of reference[14] using the program Jaguar and the LACVP** basis set. We find spin populations of 0.75 on Ni_p and 0.10 on Ni_d. If the structure is optimized, using the same geometrical constraints as in ref 14, the spins on Ni_p and Ni_d become 0.85 and 0.04, respectively, and the Ni_p-Ni_d and Ni_p-CO distances increase to 2.71 and 1.82 Å, respectively. Further optimization, but this time with the geometrical constraints that we used in our optimizations, leads to a much longer Ni_p-Ni_d distance of 2.93 Å.

Other studies have suggested that the NiFeC species contains an oxidized $[Fe_4S_4]$ cluster and a low-spin $Ni_p(II)$ with the electron located on the CO.[8,28] This led us to test two more models, $NiFeC_2$ and $NiFeC_3$. In $NiFeC_2$, the active site is in its closed form and the radical CO is positioned at the apical site. Geometry optimization leads to the same state and structure that we obtained for $NiFeC_1$ and for which there is no significant spin on CO. In $NiFeC_3$, the active site is in its open form, and the radical CO is positioned at the equatorial position. Geometry optimization gives a reduced iron−sulfur cluster, a low-spin, square-planar $Ni_p(II)$, and a CO with no spin. In all of these models, Ni_d remains in its $Ni_d(II)$ oxidation state with a square-planar conformation. Of the three models that we tested, $NiFeC_1$ is the only one that is consistent with the NiFeC signal because its spin is located on the Ni_p that is positioned between the cluster and the CO.

$Ni_p(0)/Ni_p(II)$ versus $Ni_p(I)/Ni_p(III)$. In this section, we discuss models for the initial states of the catalytic cycle depicted in Figure 1. Structure A_1, initially modeled as $[Fe_4S_4]^{2+}-Ni_p(0)$, optimized to the form $[Fe_4S_4]^{1+}-Ni_p(I)$ in which Ni_p, with a spin of −0.95, is antiferromagnetically coupled to $[Fe_4S_4]^{1+}$, with a spin of 0.89. When we compare our model to the X-ray structure, Ni_p has an almost trigonal-planar coordination, whereas experimentally the Zn_p coordination is clearly tetrahedral due to the presence of an additional unidentified ligand. A similar configuration is obtained for a calculation on the open conformation.

Webster et al.,[19] in their calculations on the A-cluster active site, suggested that the configuration $Ni_p(0)-Ni_d(II)$ was stable, but this result is probably due to the fact that they did not include the iron−sulfur cluster in their model. Synthetic model compounds also indicate that $Ni_p(0)-Ni_d(II)$ is stable,[29] but these too do not possess $[Fe_4S_4]$. The importance of the $[Fe_4S_4]$ cluster was shown by Schenker and Brunold[14] who found, like us, that its presence led to the formation of an antiferromagnetically coupled $[Fe_4S_4]^{1+}-Ni_p(I)$.

The geometry and charge-spin analyses indicate that the optimized A_1 model with $[Fe_4S_4]^{1+}-Ni_p(I)$ is stable and could be part of the catalytic cycle prior to the arrival of the substrates CO and CH_3. However, it is worth noting that all the X-ray structures have revealed four ligands for M_p; three are cysteine thiolates, but the fourth, located at about 2.5 Å from the metal, has not been clearly identified. Various suggestions have been made, including an acetate anion and a water molecule[5] or SO_2 and HCO_2^- (see ref 16) for Ni_p and an SO molecule[4] or N_3^- (see ref 16) for Zn_p.

If $[Fe_4S_4]^{2+}$ is replaced by $[Fe_4S_4]^{1+}$ in model A_1, we obtain model A_{11} which is a doublet. Optimization results in a structure in which the iron−sulfur cluster remains reduced with a spin of 1.10 and Ni_p remains zerovalent with a small residual spin of −0.10. Thus, $Ni_p(0)$ is stable next to $[Fe_4S_4]^{1+}$ but not next to $[Fe_4S_4]^{2+}$. The structure of model A_{11} is similar to that of model A_1, the major difference being in the geometry of the trigonally coordinated Ni_p which lies above the plane defined by the thiolate ligands in a configuration similar to that of the X-ray structure.

We performed a point energy calculation on larger structural models of the A_1 and A_{11} states to see if inclusion of additional interactions with the protein matrix changed the electronic structure of the active site. Because of the computational cost, only groups less than 4.0 Å from the site were included in the model which meant adding the residues Ile146, Leu508, Gly526, Leu527, Val531, Phe598, and a water molecule hydrogen-bonded to the $[Fe_4S_4]$ cluster. All dangling bonds created by extracting these groups from the crystal structure were terminated by methyl groups.

The large and small models of A_1 have similar electronic distributions. The spin on the iron−sulfur cluster ($s = 0.89$) is antiferromagnetically coupled to the spin on Ni_p ($s = -0.91$). One of the effects caused by enlarging the model is to add a hydrogen bond to the iron−sulfur cluster. This is expected to increase the redox potential of the cluster and would thereby further favor $[Fe_4S_4]^{1+}$ over $[Fe_4S_4]^{2+}$ and, consequently, $Ni_p(I)$ over $Ni_p(0)$. If residues beyond 4.0 Å from the $[Fe_4S_4]$ cluster are included, additional hydrogen bonds to three of its thiolate ligands are found (see Figure 3). Thus, in the vicinity of the active site, no residue seems to be able to reverse the tendency of the iron−sulfur cluster to be reduced more easily than $Ni_p(I)$.

The large and small models of A_{11} have similar electronic distributions, and $Ni_p(0)$, with a residual spin of −0.85, remains stable next to the reduced iron−sulfur cluster ($s = 1.63$).

(28) Funk, T.; Gu, W.; Friedrich, S.; Wang, H.; Gencic, S.; Grahame, D. A.; Cramer, S. P. *J. Am. Chem. Soc.* **2004**, *126*, 88−95.
(29) Linck, R. C.; Spahn, C. W.; Rauchfuss, T. B.; Wilson, S. R. *J. Am. Chem. Soc.* **2003**, *125*, 8700−8701.

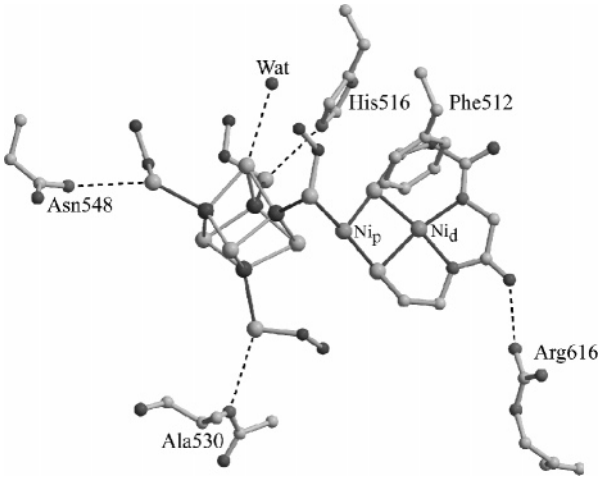

Figure 3. Hydrogen bonding interactions in the open form of ACS that involve A-cluster residues (indicated by dashed lines) and shielding of the dinuclear Ni site by Phe512.

Model A_2 was constructed to mimic the binding of CO to A_1, and like A_1, $Ni_p(0)$ is not favored as optimization leads to a species consisting of an antiferromagnetically coupled $[Fe_4S_4]^{1+}-Ni_p(I)$ pair. In contrast, in their calculations with a high-spin Fe(II) in place of the iron−sulfur cluster, Webster et al. found that binding of CO leads to breaking of the Ni_p-S_{Cys509} bond.[19]

Model A_{11} can also bind CO and give model A_{22} with a Ni_p-C_{CO} distance of 1.69 Å. However, the Ni_p-S distances are all greater than 2.5 Å, whereas those observed in the crystal structure are between 2.2 and 2.4 Å. Nevertheless, this model and A_{11} are the only ones in which $Ni_p(0)$ appears to be stable.

Gencic and Grahame proposed a mechanism involving one catalytic nickel that may be either Ni(I) or Ni(III).[8] The most oxidized state, which is not part of the catalytic cycle, was assigned as $[Fe_4S_4]^{1+}-Ni(II)$. They did not specify where the electron comes from, but they suggested an initial reduction of $[Fe_4S_4]^{1+}-Ni(II)$ to $[Fe_4S_4]^{1+}-Ni(I)$. They also did not indicate unambiguously whether Ni_p or Ni_d is catalytically relevant, although they most likely refer to Ni_p. This activated species is in agreement with the calculations of Schenker and Brunold and with our calculations on models A_1 and A_2 (see above). However, the starting electronic configuration is not silent, and there is no report of an EPR-active species for the most oxidized state of the A-cluster, A_{ox}, which is believed by most of the community to be $[Fe_4S_4]^{2+}-Ni_p(II)$. The NiFeC species, as in ref 4, is not included in the catalytic cycle, and it is viewed as an inhibited species. Here, the EPR active state is proposed to be a radical located on CO which, as we saw earlier, is not stable using our models.

Acetyl Formation. Both Gencic and Grahame[8] and Lindahl and co-workers[13,19] have proposed that methyl binds first to Ni_p in the equatorial plane, followed by CO binding and insertion to form the acetyl group. The difference between the two proposals lies in the geometry of the acetyl$-Ni_p$ complex which is square-planar (ligands are acetyl, S_{Cys509}, S_{Cys595}, and S_{Cys597}) and trigonal-planar (ligands are acetyl, S_{Cys509}, and S_{Cys595}) in the first and second mechanisms, respectively. To determine whether CH_3 or CO binds first, we calculated the energy released for a CO-free Ni_p to take the methyl from a corrinoid model (not shown) compared to a CO-bound Ni_p. We found −831 and −762 kJ mol^{-1}, respectively, which is not significant enough to discriminate the two possibilities. In their DFT calculations, Webster et al.[19] found that binding CO first led to a compound with a broken Ni_p-S_{Fe} bond (corresponding to Cys509 of Figure 2). Instead they proposed that CO binds the methylated square-planar Ni_p. It is difficult to compare this result with our data as they constructed a model of the active site, whereas we used X-ray structures as starting models.

Formation of acetyl may occur via a mononuclear or a binuclear process. We tried various hypotheses for each process and present here the most likely reaction paths that were found.

The mononuclear mechanism is represented by structures A_3 and A_4 as the reactant and the product species and by TS_M as the saddle point between them. All structures have $[Fe_4S_4]^{2+}-Ni_p(II)-Ni_d(II)$ character. Model A_3 has a distorted square-pyramidal Ni_p with CH_3 and the thiolates of cysteines 509, 595, and 597 in the plane and the CO in the apical position. Model A_4 has a square-planar Ni_p with the acetyl and the thiolates of cysteines 509, 595, and 597 as ligands. Both A_3 and A_4 were modeled in the open form of the X-ray structure. We also tried to optimize these configurations in the closed form. In the case of A_3, the optimization led to a distorted structure with a $S_{Cys509}-C_{C(O)(CH3)}-S_{Cys595}-S_{Cys597}$ dihedral of 42°, compared to 17° in the open form and Ni_p-S_{Cys509} and Ni_p-S_{Cys597} distances of 2.47 and 2.42 Å, respectively, compared to 2.35 Å for distances in the open form. This implies that there is not enough space for the methyl to occupy the equatorial site in the closed form. In the case of A_4, the acetyl adopts an equatorial position, although the structure is more distorted than in the open form, and most importantly, if we add the surrounding residues not included in our optimization, the methyl carbon is only 1.52 Å from the $C_{\delta 1}$ of residue Ile146. Adding the surrounding residues in the acetyl-bound open form leads to much steric hindrance as the closest atom is the C_ζ of residue Phe512 which is 2.77 Å away from the oxygen of the acetyl.

TS_M is a nonradical structure in which Ni_p has a distorted, square-pyramidal coordination. Compared to model A_3, the methyl group has moved most, by 2.25 Å. Significant displacements (0.4−0.8 Å) are also found for CO, Ni_p, and Cys509, with Ni_p moving in the direction of a minor site found for M_p in the crystal structure of the open form.[4] Ni_d, Cys595, and Cys597 are displaced by only 0.1−0.2 Å. One of the results of these structural changes is that the C−C distance between the CO and the CH_3 ligand has decreased from 2.85 to 1.90 Å. In addition, Ni_p now lies close to the plane that is defined by the new positions of CO (at 1.70 Å), CH_3 (at 2.15 Å), S_{Cys595} (at 2.27 Å), and S_{Cys597} (at 2.38 Å), with S_{Cys509} becoming an axial ligand (at 2.76 Å from Ni_p). The angle between this new plane and the ones described above for A_3 and A_4 is approximately 45°. The Ni_p-C-O angle is slightly bent. TS_M is 49 kJ mol^{-1} higher in energy than A_3, whereas A_4 is 83 kJ mol^{-1} more stable than A_3.

The binuclear mechanism is represented by structures A_3' and A_4', and the path models closely the mechanism proposed in refs 3 and 6, where Cu_p has been replaced by Ni_p. A_3' was initially modeled as $[Fe_4S_4]^{2+}-Ni_p(II)-CO(ax)\cdot Ni_d(II)-CH_3$, but after geometry optimization, it converged to the configuration $[Fe_4S_4]^{1+}-Ni_p(III)-CO(eq)\cdot Ni_d(II)-CH_3$ in which the spins of $Ni_p(III)$ and $[Fe_4S_4]^{1+}$ are antiferromagnetically coupled. When we were investigating the structures along the path

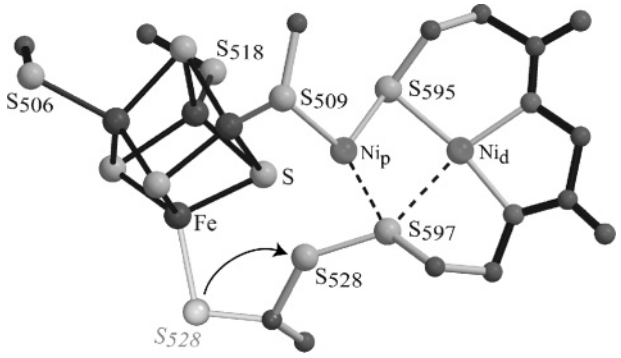

Figure 4. The A-cluster active site is shown with a putative D-site that would provide the two electrons necessary for the reaction to proceed. The X-ray model in the open form shows that a simple rotation around the $C_\alpha-C_\beta$ bond of Cys528 leads to the formation of a disulfide bond between Cys528 and Cys597. The dashed lines indicate the bonds that should be weakened by disulfide bond formation.

between A_3' and A_4', we found a lower-energy starting point that we will call A_3''. In this latter structure, the Ni_d-CH_3 distance is 2.20 Å, compared to 1.99 Å in A_3'. The most remarkable difference between A_3' and A_3'' resides in the electronic configuration. In A_3'', the iron−sulfur cluster remains oxidized and Ni_p bears a spin of 0.78 that is antiferromagnetically coupled to those of Ni_d ($s = -0.52$) and CH_3 ($s = -0.42$). This corresponds to either $[Fe_4S_4]^{2+}-Ni_p(I)-CO(eq)\cdot Ni_d(III)-CH_3$ or $[Fe_4S_4]^{2+}-Ni_p(I)-CO(eq)\cdot Ni_d(II)-$radical CH_3. Model A_3'' is 90 kJ mol^{-1} more stable than A_3', and as a result, we determined the path with A_3'' and A_4' as the end points, with TS_B as the saddle point between them. The structure of A_4' is very similar to that of A_4 except for the orientation of the acetyl group.

TS_B is composed of $Ni_d(II)$ with a radical CH_3 that is equidistant from both metals at 3.5 Å. As in A_3'', the spins of $Ni_p(I)$ and radical CH_3 are antiferromagnetically coupled and the CO, which was initially in the axial site, has moved toward the equatorial site. The rearrangement from A_3'' to TS_B is almost barrierless, whereas A_4' is more stable than TS_B by 144 kJ mol^{-1}. Nevertheless, the structures in the binuclear mechanism are less stable than those in the mononuclear mechanism, the differences being 102 and 33 kJ mol^{-1} for the pairs A_3''/A_3 and A_4'/A_4, respectively.

The binuclear mechanism implies that acetyl binds in the apical site at the proximal metal and so Ni_p is tetrahedral. However, this conformation is only stable if $Ni_p(II)$ is high spin (model not shown). A high-spin $Ni_p(II)$ was suggested by X-ray magnetic circular dichroism experiments in the as-isolated ACDS enzyme that converts into low-spin $Ni_p(II)$ upon CO binding on the reduced enzyme.[28] Optimization of a low-spin $Ni_p(II)$ complex in the open form leads to a square-planar structure in which the acetyl goes from the apical to the equatorial site, which, as mentioned above, is not favored in the closed form due to steric hindrance.

D-Site. In an early paper, Barondeau and Lindahl suggested that the two electrons necessary to drive the ACS reaction could come from disulfide bond formation between a pair of cysteines, named the D-site, in the vicinity of the A-cluster.[12] The subsequent resolution of the crystallographic structures of ACS did not directly reveal the presence of such a site, although there are a number of cysteine thiolates in the A-cluster which could potentially form a D-site (see Figure 4). One possibility, proposed recently by Svetlitchnyi et al.,[5] is a bond between the cysteines that bridges Ni_p and Ni_d. However, a closer approach of the S-atoms of these cysteines, which are 3.1 Å apart in the crystal structure, would not result in a proper geometry for a disulfide bond unless large structural distortions occur. It is also not compatible with the existing coordination geometries of the Ni ions and so appears unlikely. Inspection of the X-ray model shows two other SS-bonds to be candidates,[16] although only in the open-form structure as bond formation in the closed form would require too much structural rearrangement. Simple rotation of a cysteine side chain, without modification of the protein backbone, enables a disulfide bond to be formed between Cys528 and Cys597 or a persulfide bond between Cys528 and one of the sulfide ions from the iron−sulfur cluster.

To test these two possibilities for the D-site, we geometry-optimized models of the A-cluster with each of the SS-bonds in several different electronic states. For models with a disulfide bond between Cys528 and Cys597 (model disu1), geometry optimization of the configurations $[Fe_4S_4]^{2+}-Ni_p(0)$ and $[Fe_4S_4]^{2+}-Ni_p(0)-CO(ax)$ led to $[Fe_4S_4]^{2+}-Ni_p(II)$ and $[Fe_4S_4]^{2+}-Ni_p(II)-CO(eq)$, respectively, and a broken disulfide bond. In contrast, the configuration $[Fe_4S_4]^{2+}-Ni_p(II)-CH_3$-(eq) had a stable disulfide bond, with an S−S distance of 2.15 Å, and a square-planar Ni_p with CH_3 and three cysteine thiolates as ligands. Likewise, the configuration $[Fe_4S_4]^{2+}-Ni_p(II)-(CH_3$-(eq),CO(ax)) had a stable disulfide bond, with a length of 2.12 Å, and Ni_p adopted a slightly distorted square-planar coordination with CH_3, CO, and two cysteine thiolates as ligands. Although in both cases the disulfide bond was not broken during the optimization, this extra coordination of the sulfur of Cys597 led to the breaking of the bond between S_{Cys597} and Ni_d (about 3 Å), leaving Ni_d with only three ligands, which is not the most favorable configuration for $Ni_d(II)$.

We tested the same electronic configurations as above with a persulfide bond between Cys528 and one of the sulfide ions of the iron−sulfur cluster (model disu2). All the optimizations led the to the breaking of the bond, and the original configuration of the X-ray model was recovered, i.e., S_{Cys528} bound to an iron of the cluster. This SS-bond is thus not likely.

A possible advantage of a D-site model, compared to the other models we tested, is that no other redox reactions are needed than the one involving SS-bond formation. In addition, the overall charge of the A-cluster may be neutralized by the presence of two nearby positively charged residues, His516 and Arg616 (Figure 3). In comparison, all other models are charged negatively (Table 1).

Although this argument may favor a D-site model, it is not clear whether charge compensation is necessary to drive the reaction. We also cannot exclude the presence of positively charged ions, such as sodium ions, that are crystallographically indistinguishable from water molecules. We see two problems with the D-site model, (1) the environment of Ni_d which is less favorable than in the other structures that we examined and (2) the loss of a protein ligand to the $[Fe_4S_4]$ cluster.

Conclusion

In this paper we have examined the structural and electronic properties of a series of putative states for the A-cluster of the acetyl-CoA enzyme using density functional theory techniques. The main results of our calculations are as follows.

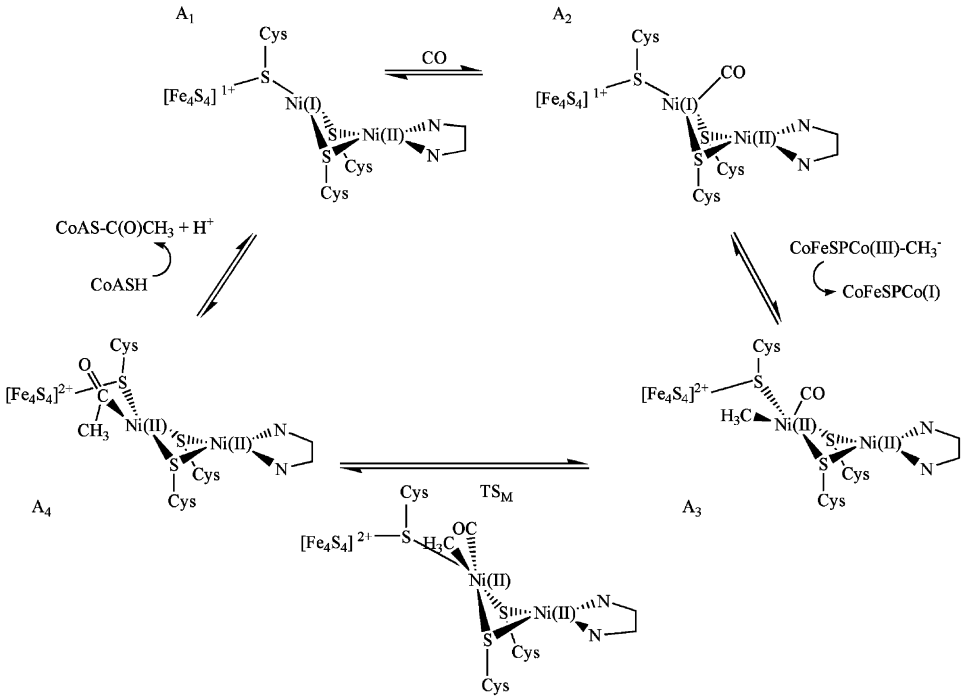

Figure 5. Possible mechanism derived from our calculations.

(1) Of the models we tested, the $NiFeC_1$ configuration, in which the spin is located on Ni_p, between the cluster and the CO, is the only one that is consistent with the NiFeC signal in which there is a broadening of the EPR signal in ^{57}Fe, ^{61}Ni, and ^{13}CO experiments.[30] Indeed, it is likely that if the radical were located on the CO or on the $[Fe_4S_4]$ cluster, isotopic perturbation with ^{57}Fe or ^{61}Ni, respectively, would not be significant.

(2) In most of our calculations, the distal nickel remains in the $Ni_d(II)$ ($s = 0$) form. This is consistent with the X-ray models of the open and closed conformations in which the environment of Ni_d does not change. The exceptions concern structures that are involved in the binuclear mechanism for acetyl formation, but our calculations suggest that this is not favored (see below).

(3) The zerovalent state proposed for Ni_p is stabilized only by a neighboring reduced iron−sulfur cluster ($s = {}^1/_2$). Enlarging the model of the active site with neighboring residues does not alter this electronic configuration. Upon CO binding, $Ni_p(0)$ is still favored next to the $s = {}^1/_2$ cluster. Next to $[Fe_4S_4]^{2+}$, $Ni_p(0)$ is oxidized to $Ni_p(I)$. Enlargement of the model adds hydrogen bonds to the $[Fe_4S_4]$ cluster and reinforces its tendency to be reduced to $[Fe_4S_4]^{1+}$ and, consequently, for $Ni_p(0)$ to be oxidized to $Ni_p(I)$.

(4) The mononuclear mechanism for acetyl formation appears to be favored over the binuclear mechanism primarily because the structures involved are more stable.

(5) The existence of a D-site involving Cys528 and Cys597 is possible. Our calculations suggest that only the approach of a CH_3 cation can trigger the formation of this disulfide bond. Although this bond is stable, the structures that we obtain are significantly distorted compared to the ones without this bond, especially at Ni_d.

A plausible catalytic cycle consists of the models A_1, A_2, A_3, and A_4 (see Figure 5). This means that in the initial stages of the cycle the iron−sulfur cluster is reduced, whereas in the latter stages it is oxidized. This contradicts recent observations of Tan et al. indicating that the methylation of the enzyme is over 100 times faster than the reduction of the cluster.[15] These authors favor CH_3, and not CO, binding first to the metal because they believe the NiFeC state does not belong to the catalytic cycle.[12]

The mechanism consisting of the structures A_{11}, A_{22}, A_{33}, and A_{44} can be questioned because these structures are EPR-active and no EPR signal has been detected in the catalytic cycle. This mechanism corresponds to the one originally proposed in reference[4] but with the iron−sulfur cluster in its reduced form. The same reasoning also casts doubt on the involvement of NiFeC in catalysis.

Two of us (AV, JFC) have put forward a "gating mechanism" in which CO binds first in the closed form because it is in this form that the tunnel to the C-cluster is open allowing CO access to Ni_p. The structure would then open preventing CO from escaping to the medium via the A-cluster (CO is an inhibitor of many metalloenzymes) and allowing CoFeSP to transfer methyl to the equatorial position of Ni_p in the A-cluster.[16] If this scenario were true, it would, in vivo, disfavor any mechanism in which methyl binds first because the C-cluster tunnel would be blocked and the second substrate, CO, could not access the active site. Barondeau and Lindahl[12] justify the binding of methyl prior to CO by the fact that when they add CO to the native enzyme they form what they called the "nonfunctional A_{red}-CO state" (the NiFeC species). However, Ragsdale and co-workers have argued that the NiFeC species is catalytically competent and that the order of substrate binding is random.[17,31] Unless the X-ray structure of the corrinoid

(30) Fan, C. L.; Gorst, C. M.; Ragsdale, S. W.; Hoffman, B. M. *Biochemistry* **1991**, *30*, 431−435.

protein/ACS complex becomes available, it is hard to imagine a calculation that will unequivocally discriminate between these possibilities.

Acknowledgment. The authors thank the Commissariat à l'Energie Atomique and the Centre National de la Recherche Scientifique for support of this work. P.A. and M.J.F. would also like to thank Dr. Jean-Marie Mouesca for helpful discussions.

JA0439221

(31) Gorst, C. M.; Ragsdale, S. W. *J. Biol. Chem.* **1991**, *266*, 20687−20693.